SEISMIC RESPONSES OF STRUCTURES SUBJECTED TO INCIDENT INCOHERENT WAVES CONSIDERING A LAYERED MEDIA WITH IRREGULAR INTERFACES

Katsuhisa KANDA[1]

SUMMARY

The spatial coherency and amplitude characteristics of ground motions are analyzed using a two-dimensional FEM model to consider a layered medium with irregular interfaces. The analytical results show that the interface irregularities between layers spatially change the frequency characteristics of ground motions on the soil surface. If the spatial variation of incident waves is considered according to a spatial coherency function derived from observed data, the ground motions show different characteristics. The amplitude of horizontal ground motions subjected to spatially varying incident waves reduces compared to vertically incident plane waves. The vertical ground motions depend on a layered medium with irregular interfaces and spatial variation of incident waves. The irregular interfaces influence the spatial variation of ground motion and alter its coherency function. The responses of a building with a rigid raft foundation are evaluated for an average earthquake. The analytical results suggest that the response reduction rates due to the soil-structure effect and spatial incoherence effect of incident waves are almost equal. The rocking input motion related to vertical ground motions affect the horizontal responses of buildings. The spatial variation effect for structural responses depends on the natural frequency of a building and the size of its foundation. It concludes that the effect of the spatial incoherence of incident waves and a layered medium with irregular interfaces on ground motions and structural responses can not be negligible.

INTRODUCTION

The soil under a building often shows irregularities in the horizontal interfaces between soil layers. In such a case, one-dimensional soil profiles are insufficient to analyze the soil amplification characteristics. The incident seismic waves propagate with refraction and reflection at irregular interfaces and give spatial variation to the amplitude and frequency characteristics of ground motions. Though the effect of irregular interfaces between layers is significant, that of heterogeneous media in the layer may be omitted in the local site-response problem [Kanda et al. 1995]. The spatial variation of incident waves has been stochastically characterized by the coherency function. The interface irregularities reduce the spatial coherency of ground motions due to the superposition of phase-lagged incident waves. The reduction of spatial coherency has been analyzed by a lot of researchers using data observed at dense seismic arrays. It has been revealed that spatial coherency shows some form of exponential decay or a double exponential decay with frequency and separation distance [Abrahamson et al 1991, Vanmarcke 1984]. However, there are different characteristics in the spatial coherency of ground motions recorded by strong motion arrays located on approximately horizontally layered soil, such as the Lotung LSST array, and those located on topographically irregular soil, such as the USGS Parkfield array [Schneider et al. 1992]. The spatial coherency at a topographically irregular site tends to be less dependent on frequency [Kanda 1998, Zerva et al. 1997].

The spatial variation influences not only ground motions but also structural responses. It is well known that spatial variation of incident waves decreases the translational response and increases rocking and torsional responses of rigid extended foundations [Luco et. al. 1986]. Furthermore, the response characteristics of superstructures are closely related to the soil-structure interaction, and the natural frequency and damping of the

[1] *Kobori Research Complex, Kajima Corporation, 107-8502 Tokyo, Japan Email: kanda@krc.kajima.co.jp*

superstructures. It is significant to quantify the effect of spatial variation of incident waves on structural response. The effect of spatial variation on ground motions and structural response is herein denoted as incoherence effect.

This paper discusses the structural response and ground motion characteristics such as amplitude and coherency considering a layered medium with irregular interfaces. The two-dimensional finite element method (FEM) is employed to model a layered medium with irregular interfaces. An exponential-type smooth coherency function decayed over frequency and distance is used as the incoherent incident wave. In addition, the covariance analysis using three-dimensional soil-structure analytical representations is carried out for the parametric study of structure response.

SPATIAL VARIATION OF GROUND MOTIONS

Analytical Conditions and Methodology

FEM analyses are employed with the viscous boundary at the bottom and the transmitting boundary at the side of finite elements. If the incident waves along the bottom boundary are given, the responses of the finite element region can be calculated. A cross-spectral density function of incoherent incident waves between i (x_i, z_i) and j (x_j, z_j) is defined with exponential-type coherency as follows:

$$s_{ij} = \cos\left(\frac{\omega z_i}{Vs}\right)\cos\left(\frac{\omega z_j}{Vs}\right)\exp\left(-\frac{\gamma\omega\left|x_i - x_j\right|}{Vs}\right)s_0(\omega) \tag{1}$$

where Vs is shear wave velocity of half space, γ is a coefficient of coherency decay, and $s_0(\omega)$ is a power-spectral density function of the incident waves. This equation considers the incoherence of incident waves only in the horizontal direction x. The incident waves at the boundaries are generated as a one-dimensional, multi-variate random process in the x direction [Shinozuka 1985]. The cross-spectral density matrix $[S_f]$ whose elements are shown in eqn.(1) is decomposed into a lower triangular matrix $F(\omega_m)$ as follows:

$$\left[S_f(\omega_m)\right] = \left[F(\omega_m)\right]\ \left[F(\omega_m)\right]^T \tag{2}$$

Once $[F(\omega_m)]$ of the m th discrete circular frequency ω_m is obtained, a set of n homogeneous processes of incident wave $U_{fl}(\omega_m)$ can be simulated by the following series:

$$U_{fl}(\omega_m) = \frac{\sum_{k=1}^{l} F_{lk}(\omega_m)\cos(\phi_{km})}{F_{11}(\omega_m)\cos(\phi_{1m})}U_{f1}(\omega_m) \qquad l = 1,2,..n \tag{3}$$

where $\phi_1, \phi_2, ...\phi_n$ are independent random phase angles distributed uniformly over the range $(0,2\pi)$, $F_{lk}(\omega_m)$ is an element of matrix $[F(\omega_m)]$, and $U_{f1}(\omega_m)$ is a given incident wave at an initial point.

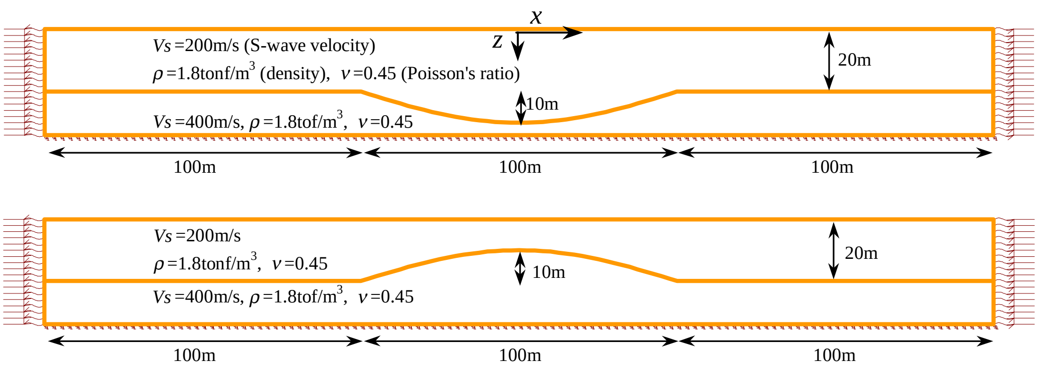

Figure 1: FEM models for irregular layer interfaces (upper: concave layer, lower: convex layer)

It is difficult to determine the lateral interface irregularities in detail due to the lack of geological data. The analytical models are simplified and contain two layers. Concave and convex sine-shaped interfaces are assumed between the layers, as shown in Figure 1. The material damping ratio for soil is 3%. First, the ground motions on the surface are computed for a vertically incident plane SV wave.

Amplitude of Ground Motions

Figure 2 shows the horizaontal displacement normalzed by the vertically incident SV-wave at five different points on the soil surface. The frequency characteristics of displacements are significantly variable spatially due to layer irregularities. The frequencies of peaks and troughs in the displacement above the concave interface get lower compared to those above the horizontal layer. The convex layer shows the opposite tendency.

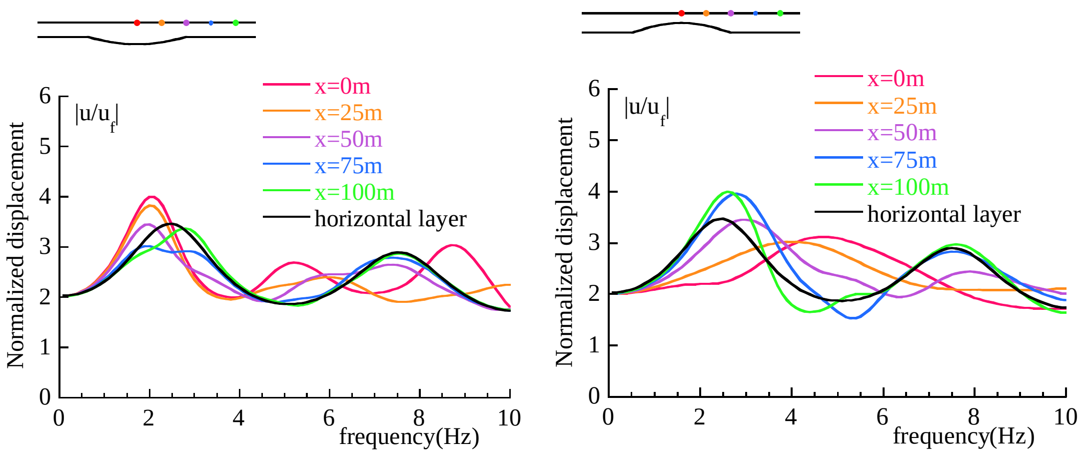

(a) concave layer **(b) convex layer**

Figure 2: Normalized displacements of soil surface for coherent plane wave (SV-wave)

The power spectrum $G(\omega)$ of incident waves is modeled by equation (4), whose parameters are determined by fitting to the average spectrum of 20 incident waves normalized at 100cm/s^2 maximum acceleration observed at Kushiro (GL-22m) [Kanda 1998], where $\omega_0=3\pi$, $\omega_r=6\pi$ and α is the maximum acceleration, as shown in Figure 3(a).

$$G(\omega)=\left(\frac{\alpha}{2.4}\right)^2 \frac{1}{\omega_r\left(1+(\omega_0/\omega)^2\right)^2}\exp\left(-\frac{\omega}{\omega_r}\right) \tag{4}$$

Since there are no shallow and near-field events in the observed data, the wave-passage effect and extended source effect in incoherent incident waves may be neglected. The variation of spectrum is relatively small [Kanda 1998]. As the coherency function for incohrent incident waves is assumed to decline to 0.5 with a wavelength [Toksöz et al. 1992], the coefficient of coherency decay γ in equation (1) is evaluated as shown in Figure 3(b).

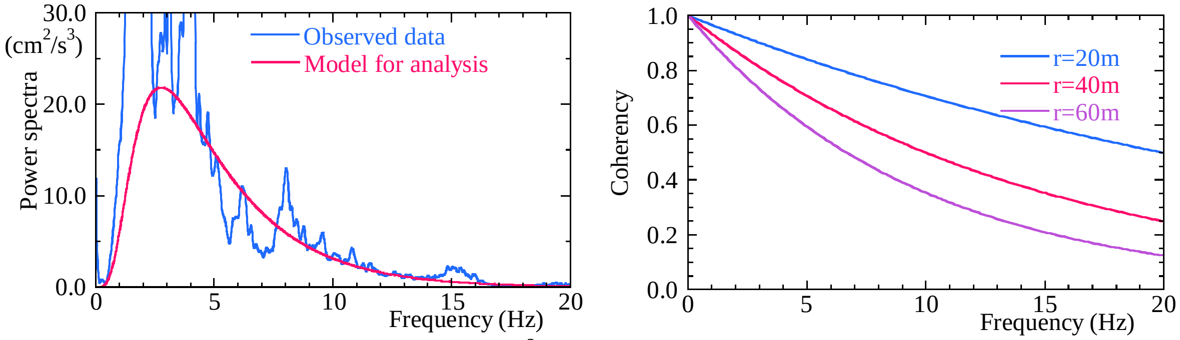

(a) Power spectral density function (100cm/sec^2) **(b) Coherency function for separation distance *r***

Figure 3: Modeling of incident wave

A sample of incoherent incident waves is simulated by equation (3). The power spectra $G_s(\omega)$ of the response at the soil surface are calculated using the FEM model (Figure 1). The root-mean-square (RMS) of acceleration representing an average response is given by:

$$\sigma = \sqrt{\sum_{i=1}^{\infty} G_s(\omega)\Delta\omega} \tag{5}$$

Figure 4 shows the RMS distribution of acceleration of the soil surface in terms of horizontal distance x from the center of the model. The horizontal displacement generated by a spatial variable wave (denoted as incoheret) is less than that by a vertical plane wave (denoted as coherent). No vertcal ground motions are generated by a coherent wave at the soil surface in horizontally layerd soil (denoted as straight), but they are generated in topographically irregular soil or by an incoherent wave.

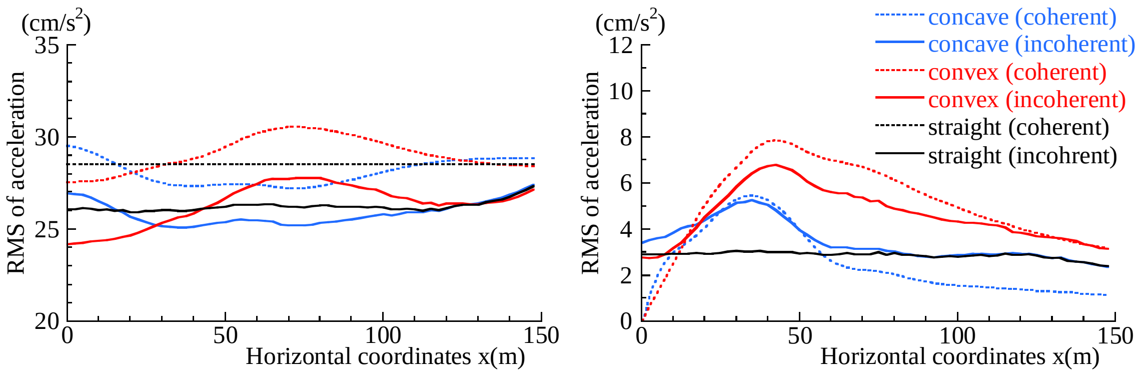

(a) Horizontal component **(b) Vertical component**

Figure 4: Root-mean-squares of acceleration of soil surface

Spatial Coherency of Ground Motions

Figure 5 shows the spatial coherency coh_{12} of ground motions between the two points (d=20m: x=-10m and 10m, d=40m: x=-20m and 20m) defined using a smoothed cross spectrum S_{ij} by equation (6).

$$coh_{12} = \frac{|S_{12}|}{\sqrt{S_{11}S_{22}}} \tag{6}$$

The coherency at low frequencies is almost one. However, the coherency at higher than a peak frequency of 2.5Hz fluctuates corresponding to the irregular interfaces. The coherency of response mostly increases at low frequencies compared to that of the incident wave shown in Figure 3(b).

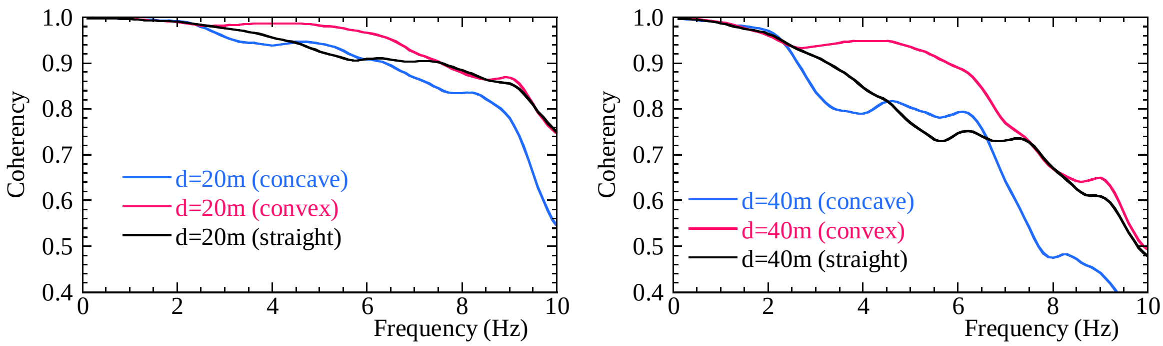

Figure 5: Coherence function of two separation distances due to layer irregularities

Structural Response Using Two-dimensional FEM Analysis

To quantify the effects of spatial variation of incident waves on the responses of buildings with rigid foundations at topographically irregular sites, the FEM analytical model with a mass structure and a rigid massless beam foundation is considered, as shown in Figure 6. If the fixed base natural period of the building is T_0(s), the building mass is assumed to be 500*T_0(ton) for unit depth, and the height of building mass is 25*T_0(m).

First, the case of coherent incident waves is considered. Figure 7 compares the RMS accelerations of translational responses of the foundation and building with those of the free soil surface without a building. The discrepancy between 'foundation' and 'free soil surface' shows the effects of soil-structure interaction. The building's response depends on its natural period. It becomes maximum where the predominant period of the surface layer corresponds to the building's natural period.

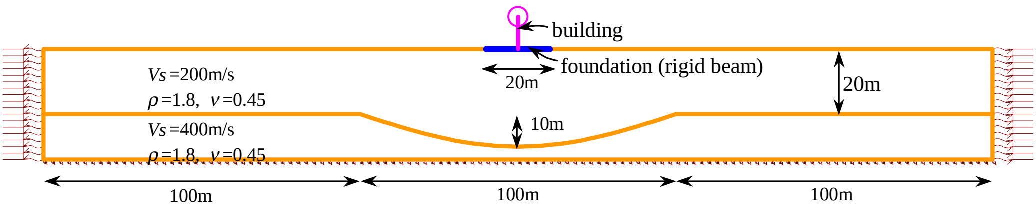

Figure 6: FEM model for the analysis of structural responses (concave case)

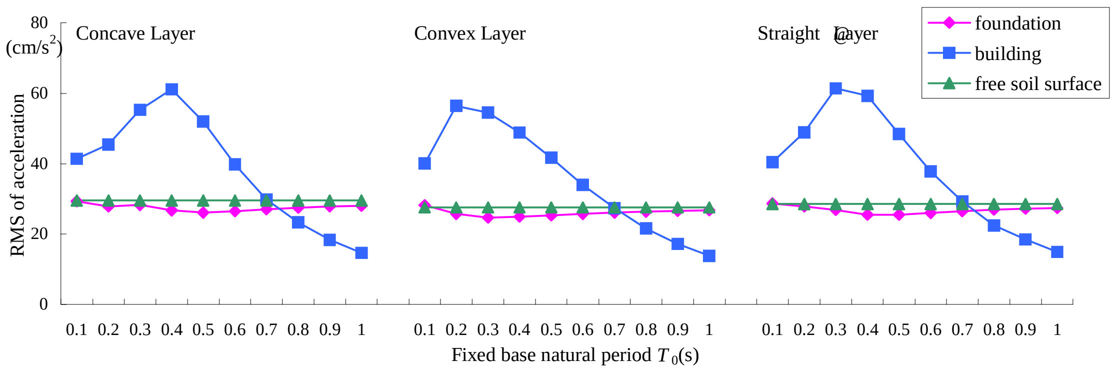

Figure 7: RMS of acceleration response for coherent incident wave

Figure 8 compares the RMS of translational accelerations for a building whose natural period is 0.4s in terms of incident wave type and nonhorizontally layered structure. The results suggest that the soil-structure interaction effect reduces about 10% of the response and the spatial incoherence effect of the incident wave reduces about an additional 10% of the response at the foundation. However, the decrease in the building's response is 7 or 8%. The discrepancy in the reduction rate may be attributed to the rocking motion of the building. These reduction rates are similar for various types of interface irregularities.

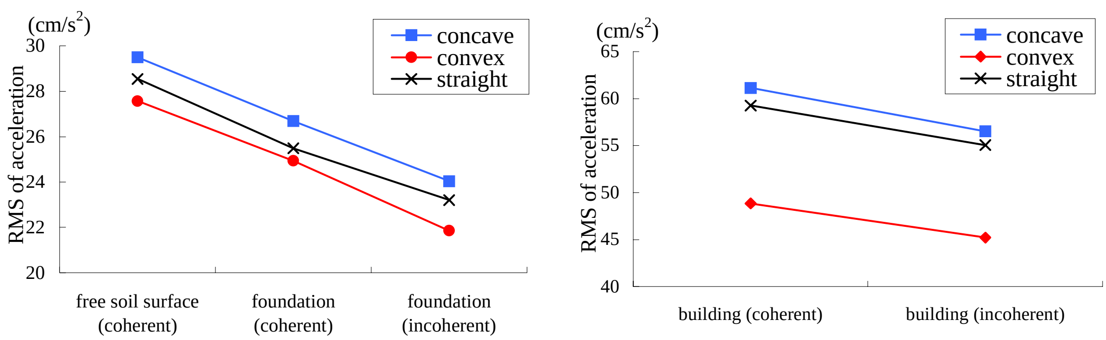

Figure 8: Comparison of horizontal accelerations between coherent and incoherent incident waves (T_0=0.4s)

Figure 9 shows the RMS distribution of vertical acceleration at the foundation. The vertical motions are generated at the center (x=0m) of the foundation for the incoherent incident waves. The vertical motions at the edge (x=10m) of the foundation are reduced by about 6%. This suggests that the reduction effect due to incoherent incident waves of rocking motion is smaller than that of horizontal motions.

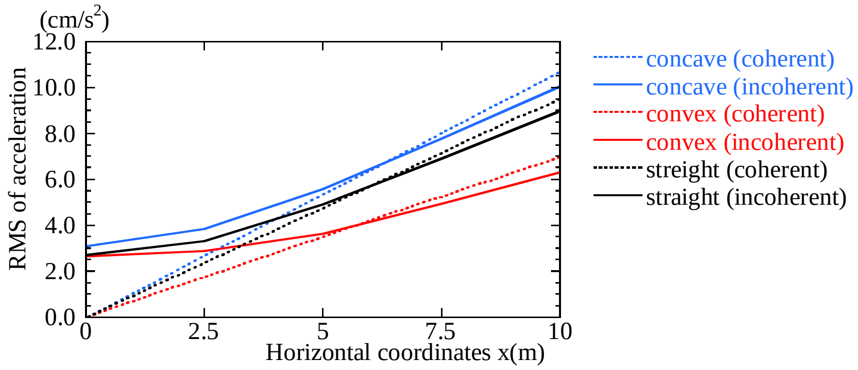

Figure 9: Comparison of vertical acceleration on foundations between coherent and incoherent incident waves (T_0=0.4s)

Structural Response Using Three-dimensional Analysis

The three-dimensional effect of incoherent incident waves on structural response is quantified. The analytical model is shown in Figure 10. A superstructure with a square rigid foundation is idealized in the same manner as in Figure 6. The foundation is in contact with the half space soil whose profiles are Vs=200m/s, ρ=1.8tonf/m^3, and ν=0.45.

$$\left(-\omega^2[M]+i\omega[C]+[K]\right)\{U\}=\{F'\} \tag{7}$$

where $\{U\}=\{x_1 \quad x_0 \quad \theta\}^T$: displacement vector, $\{F'\}=\{0 \quad F_1 \quad F_5\}^T$: part of 6 DOF driving force vector $\{F\}$, $[M]$: mass matrix, $[C]$: damping matrix, and $[K]$: stiffness matrix. If $[S]=\left(-\omega^2[M]+i\omega[C]+[K]\right)$ is used, the covariance matrix $[Q]$ is written as equation (8). The tilde denotes a complex conjugate.

$$[Q]=\{U\}\{\tilde{U}\}^T=[S]^{-1}\{F'\}\{\tilde{F}'\}^T\left[\tilde{S}\right]^{-1T} \tag{8}$$

The covariance matrix $[D]$ of the driving force vector $\{F\}$ can be expressed using the cross spectrum matrix $[G]$ of free-field motions for the contact area between the foundation and soil as follows:

$$[D]=\{F\}\{\tilde{F}\}^T=[T]^T[\Lambda]\,[G]\,\left[\tilde{\Lambda}\right]\,[T] \tag{9}$$

where $[\Lambda]$ is the total impedance matrix for the contact area between the foundation and the soil, and $[T]$ is the rigid-body motion influence matrix. The cross spectrum matrix $[G]$ is assumed to be the same as in equation (1). If the elements of [D] calculated by equation (9) are substituted into equation (8), the covariance of structural response can be evaluated.

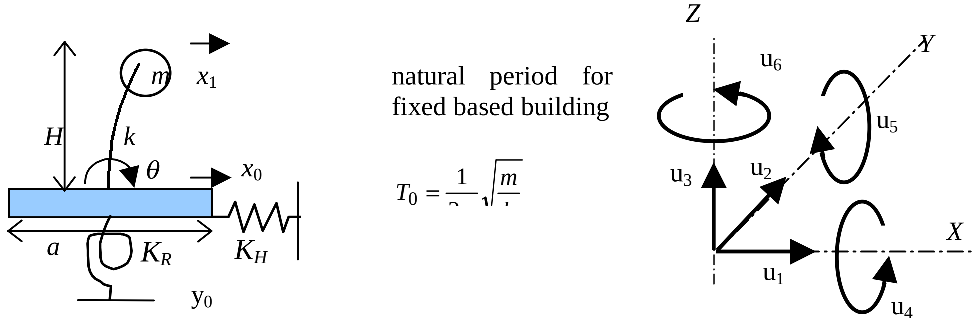

Figure 10: Structural response analysis model

Figure 11 shows foundation input motions for a massless rigid foundation. The free-field motion is spatially variable in the X and Y directions. Although the horizontal components reduce at high frequencies, vertical, rotational and torsional components are generated.

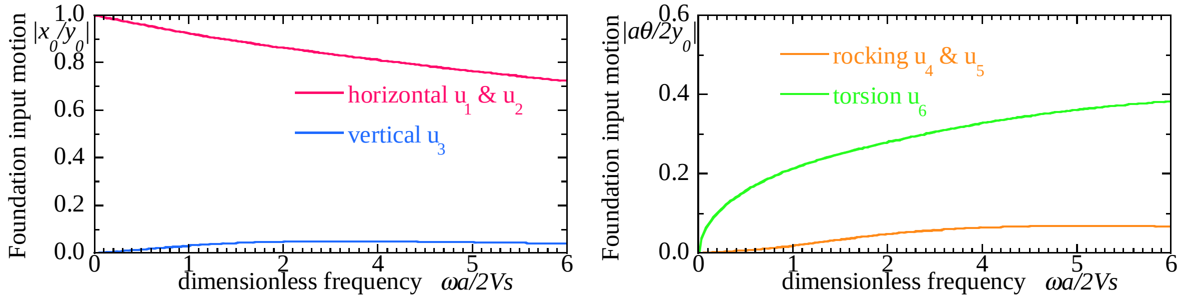

(a) lateral motion **(b) rotational motion**

Figure 11: Foundation input motion for massless rigid foudation (*ν*=0.45)

The superstructure responses are evaluated in terms of fixed base natural period T_0=0.1~1.0s. Figure 12 shows the absolute amplitude of the responses normalized by that of the free-field motions. The case of incoherent free-field motion is denoted herein as 'incoherent' and the case of a vertically incident plane S wave is denoted herein as 'coherent'. The responses of the incoherent case are smaller than those of the coherent case. Since the horizontal foundation input motion decreases with higher frequencies, the difference between superstructure responses of coherent and incoherent motions increases at high frequencies.

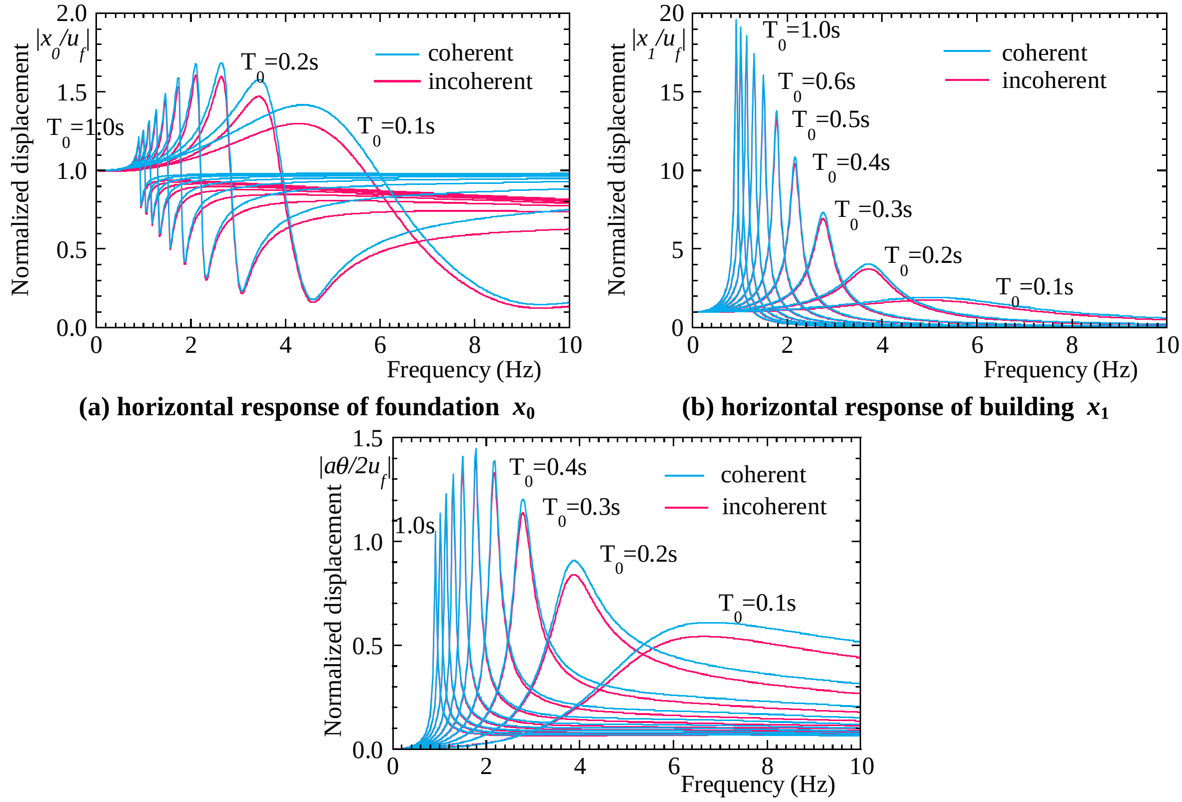

(a) horizontal response of foundation x_0 **(b) horizontal response of building** x_1

(c) rotational response of building θ

Figure 12: Normalized response of buildings in terms of T_0**=0.1-1.0 second (*a*=20m)**

The free-field motion is assumed to be the same as for the incident wave model shown in Figure 3. The RMS acceleration of the structural response is evaluated. The response reduction rates for the incoherent case to the coherent case are shown as functions of building natural period and foundation width in Figure 13. The building's response reduces with the decrease in fixed-base natural period and with the increase in foundation width. Although the foundation response decreases with the increase in foundation width in the same manner, it has less dependency on the fixed-base natural period. The average reduction rate for the foundation is about 4% for a=10m, 8% for a=20m and 16% for a=40m. However, the average reduction rate for the building is about 2% for a=10m, 4% for a=20m and 9% for a=40m. The reduction rate is small compared to the two-dimensional case in Figure 8, because the two-dimensional case includes the incoherence effect due to wave propagation in the surface layer.

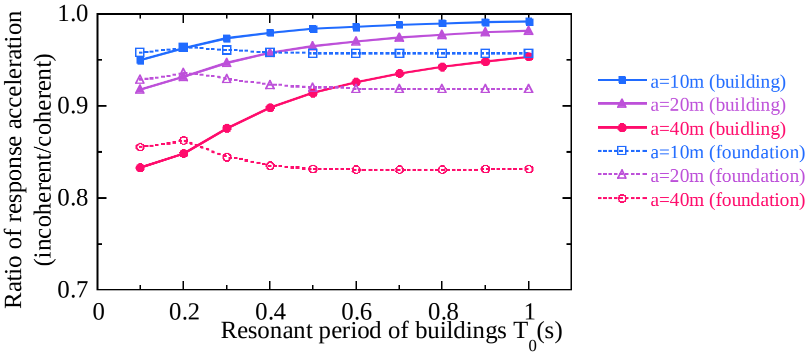

Figure 13: Ratio of RMS of response accelerations between incoherent and coherent cases

CONCLUSIONS

1. Interface irregularities between layers significantly change the frequency characteristics of ground motions at the soil surface.
2. The spatial variable incident wave reduces horizontal ground motions and produces vertical motions where no vertical motions occur for the vertical incident plane wave.
3. Although the spatial coherency of ground motion is nearly unity at frequencies lower than the first predominant frequency of the soil, it fluctuates and depends on the types of irregular interfaces at high frequencies.
4. The response of a structure with a rigid raft foundation subjected to spatially variable incident waves decreases compared to the case of vertical incident plane waves. The incoherence effect increases as frequency increases.
5. The reduction rate due to the incoherence effect on the foundation response is about 10% and is equivalent to the soil-structure interaction effect. The reduction rate of the building response due to the incoherence effect is smaller than that of the foundation response. The reduction rate of the building and foundation depends on the fixed-base natural period of the building and the size of the foundation. The reduction rate is similar, depending on the type of irregular interfaces.

ACKNOWLEDGMENT

Informative discussion with Prof. Y. Inoue, Osaka University, Prof. M. Motosaka, Tohoku University, and Dr. K. Miura, Kobori Research Complex, is gratefully acknowledged.

REFERENCES

Abrahamson, N., Schneider, J.F. and Stepp, J.C. (1991), "Empirical spatial coherency functions for application to soil-structure interaction analyses", *Earthquake Spectra*, 7, 1, pp1-27

Kanda, K. (1998), "Spatial incoherence and amplitude characteristics of ground motions in surface layers with topographic irregularities", *Proc. Second International Symposium on the Effects of Surface Geology on Seismic Motion*, 2, pp.1191-1204

Kanda, K. and Motosaka, M. (1995), "Analysis on amplification characteristics of ground motion in topographic irregular site subjected to spatially varying incident wave", *J. Struct. Constr. Eng., AIJ*, 495, pp79-86

Luco, J.E. and Wong, H.L. (1986), "Response of a rigid foundation to a spatially random ground motion", *Earthquake Engineering and Structural Dynamics*, 14, pp891-908.

Schneider, J.F., Stepp, J.C. and Abrahamson, N.A. (1992), "The spatial variation of earthquake ground motion and effects of local site condition", *Proc. 10th WCEE*, 2, pp.967-972

Shinozuka M. (1985), "Stochastic fields and their digital simulation", *Lecture notes for CISM course on Stochastic Methods in Struct. Mech.*, Udine, Italy

Toksöz, M.N., Dainty, A.M. and Coates, R. (1992), "Effects of lateral heterogeneity on seismic motion", *Proc. First International Symposium on the Effects of Surface Geology on Seismic Motion*, pp33-64

Vanmarcke, E. H. (1984), *Random Fields, Analysis and Synthesis*, MIT Press

Zerva, A. and Harada T. (1997), "Effect of surface layer stochasticity on seismic ground motion coherence and strain estimates", *Soil Dynamics and Earthquake Engineering*, 16, pp445-457